

## Half-metallic ferromagnetism: Example of CrO<sub>2</sub> (invited)

J. M. D. Coey and M. Venkatesan

*Physics Department, Trinity College, Dublin 2, Ireland*

A broad classification scheme is proposed for half-metallic ferromagnets which embraces the possibilities of itinerant and localized electrons, as well as semimetallic and semiconducting electronic structure. Examples of each type are given. The problems of defining and measuring spin polarization are discussed and some characteristics of half-metals are reviewed with reference to chromium dioxide. © 2002 American Institute of Physics. [DOI: 10.1063/1.1447879]

### I. HALF METALS

A half metal is a solid with an unusual electronic structure. For electrons of one spin it is a metal with a Fermi surface, but for the opposite spin there is a gap in the spin-polarized density of states, like a semiconductor or insulator. This definition presupposes a magnetically ordered state to define the spin quantization axis. The responses of a half metal to electric and magnetic field at zero temperature are quite different. There is electric conductivity, but no high-field magnetic susceptibility.<sup>1</sup>

Normal ferromagnets, even strong ferromagnets, are not half metals. Cobalt and nickel have fully spin-polarized *d*-bands with a filled  $\uparrow 3d$  band and only  $\downarrow d$  electrons at the Fermi level  $E_F$ . However, the Fermi level also crosses the unpolarized *4s* band, so there is a density of both  $\uparrow$  and  $\downarrow$  electrons there. In order to obtain only  $\uparrow$  or  $\downarrow$  electrons at  $E_F$ , it is necessary to reorder the *3d* and *4s* bands by hybridization, pushing the bottom of the *4s* band up above  $E_F$  or depressing the Fermi level in the *d*-band below the bottom of the *4s* band. Otherwise a hybridization gap might be introduced at  $E_F$  for one spin orientation. In any case, it is necessary to pass from a pure element to an alloy or compound; all half metals contain more than one element. Most known examples are oxides, sulfides or Heusler alloys. Some are stoichiometric compounds, others are solid solutions.

Two situations where there is a single spin orientation at  $E_F$  are illustrated in Fig. 1. In either case there is a spin gap  $\Delta_{\downarrow}$  or  $\Delta_{\uparrow}$  and a smaller gap  $\Delta_{sf}$  for spin-flip excitations from the Fermi level. Half-metallic oxides where the *4s* states are pushed above  $E_F$  by hybridization with the O(*2p*) states are type I<sub>A</sub> when there are less than five *d* electrons, but of type I<sub>B</sub> when there are more than five. Otherwise, half-metallic Heusler alloys with heavy *p* elements like Sb tend to have the *3d* levels depressed below the *4s* band edge by *p-d* hybridization. CrO<sub>2</sub> is a type I<sub>A</sub> half metal with  $\uparrow$  electrons of mainly Cr(*t<sub>2g</sub>*) character at  $E_F$ .<sup>2</sup> Another well-known example is the half Heusler alloy NiMnSb<sup>3</sup> which has  $\uparrow$  electrons of Ni(*e<sub>g</sub>*) character at  $E_F$ . A type I<sub>B</sub> half-metallic oxide is Sr<sub>2</sub>FeMoO<sub>6</sub>,<sup>4</sup> where the  $\downarrow$  conduction electrons are mainly of Mo(*t<sub>2g</sub>*) character. The Heusler alloy Mn<sub>2</sub>VAl<sup>5</sup> which has Mn(*t<sub>2g</sub>*)  $\downarrow$  electrons at  $E_F$  is another type I<sub>B</sub>.

Electrons in the second class, type II half metals, lie in a band that is sufficiently narrow for them to be localized. The heavy carriers may form polarons and conduction is then by hopping from one site to another with the same spin. Other-

wise, the states in band tails may be localized by the presence of disorder; there is then a mobility edge, and conduction involves excitation to that edge. In either case, there is activated conduction  $\rho \approx \rho_{\infty} \exp(E_a/kT)$  with  $E_a \approx 0.1$  eV. Magnetite, the best-known example,<sup>6</sup> is a type II<sub>B</sub> half metal where  $\downarrow$  electrons of Fe(*t<sub>2g</sub>*) character hop among *B* sites in the spinel structure.

A third class of half metals, known as the transport half metals,<sup>7</sup> have localized  $\uparrow$  carriers and delocalized  $\downarrow$  carriers or *vice versa*. A density of states exists for *both* sub-bands at  $E_F$ , but the carriers in one band have a much larger effective mass than those in the other. So far as electronic transport properties are concerned, only one sort of carriers contributes significantly to the conduction. A schematic band structure of type III<sub>A</sub> is shown in Fig. 2(a). The heavy carriers give an activated conduction but they are short circuited by the light carriers which are metallic, with resistivity given by Matthiessen's rule  $\rho \approx \rho_0 + \rho(T)$ . An example of type III<sub>A</sub> is the optimally doped manganite (La<sub>0.7</sub>Sr<sub>0.3</sub>)MnO<sub>3</sub>, with mobile Mn(*e<sub>g</sub>*)  $\uparrow$  electrons and immobile Mn(*t<sub>2g</sub>*)  $\downarrow$  electrons at  $E_F$ .<sup>7</sup>

There is a big difference between a half metal and a semimetal. A semimetal, of which bismuth is the textbook example, is usually nonmagnetic with small and equal numbers of electrons and holes ( $\approx 0.01$  per atom) due to a fortuitously small overlap between valence and conduction bands [Fig. 2(b)]. However, if a semimetal is magnetically ordered with a great disparity in effective mass between electrons

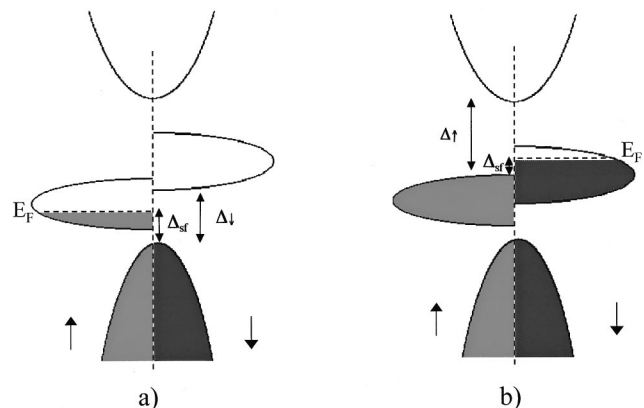


FIG. 1. Schematic density of states for a half metal, (a) Type I<sub>A</sub> with only  $\uparrow$  electrons at  $E_F$  and (b) Type I<sub>B</sub> with only  $\downarrow$  electrons at  $E_F$ . In narrow *d* bands, the states at  $E_F$  may be localized (type II).

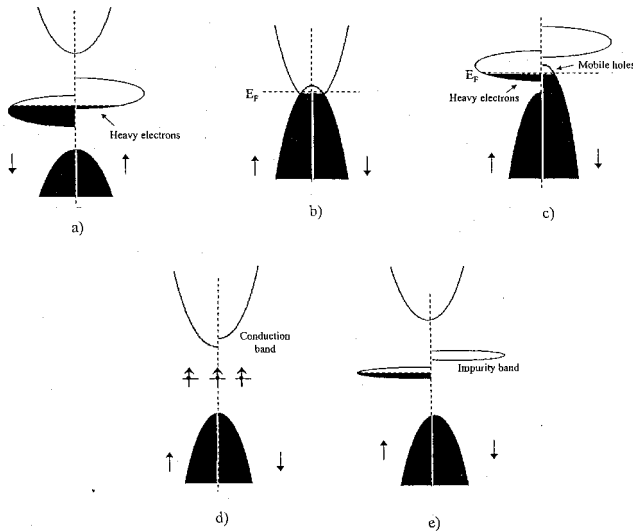


FIG. 2. Schematic density of states for (a) a type III<sub>A</sub> half metal, where electrons of one spin direction are itinerant and the others are localized, (b) a semimetal, (c) a type IV<sub>A</sub> half metal, and (d), (e) two types of ferromagnetic semiconductor.

and holes, it may be a type IV half metal. An example is  $\text{Ti}_2\text{Mn}_2\text{O}_7$ ,<sup>8</sup> [Fig. 2(c)], where a few heavy  $\uparrow$  Mn holes lie at the top of the Mn( $e_g$ ) band, while there is an equal number of light  $\downarrow$  electrons of mainly Ti(6s) character.

Finally, we consider the electronic structure of ferromagnetic semiconductors. These can become half metallic in one of two ways: In one case, localized ion cores may polarize the conduction or valence band by  $s\text{-}S$  exchange, producing a spin splitting which is greater than the Fermi energy. Examples are EuO and EuS doped with  $R^{3+}$ , where the  $4f^7$   $\text{Eu}^{2+}$  ion cores split the bottom of the  $5d/6s$  conduction band by about 0.2 eV,<sup>9</sup> and (GaMn)As where  $d^5$   $\text{Mn}^{2+}$  cores split the top of the valence band, producing  $\downarrow$  holes.<sup>10</sup> Another possibility is that the dopant impurity atoms lie sufficiently close to each other to form a narrow band which is unstable with respect to spin splitting. None of the atoms need then be magnetic. It is possible that  $(\text{La}_{0.005}\text{Ca}_{0.995})\text{B}_6$  and ferromagnetic carbon belong to this category.

Our classification is summarized in Table I. Prospects for discovering new half-metallic compounds are quite limited, but the prospects are better for finding new solid solutions with robust half metallicity.<sup>11</sup>

Half metallicity is not easy to detect experimentally. Unlike superconductors, metals, semiconductors or insulators, there is no clear electrical signature. It is impractical to measure the intrinsic high-field susceptibility of a ferromagnet at low temperature sufficiently accurately to assert that it is zero. The best indication of a type I or type II half metal is metallic conduction in a solid with a spin moment at  $T=0$  which is *precisely an integral number of Bohr magnetons per unit cell*. In a stoichiometric compound, the number of electrons per unit cell  $n = n^\uparrow + n^\downarrow$  is an integer. On account of the gap in one of the spin-polarized bands,  $n^\uparrow$  or  $n^\downarrow$  is also an integer. It follows that both  $n^\uparrow$  and  $n^\downarrow$  are integers, and so then is the difference  $n^\uparrow - n^\downarrow$  which is the spin moment in

TABLE I. Summary of the classification of half-metals.

Type	Density of states	Conductivity	$\uparrow$ electrons at $E_F$	$\downarrow$ electrons at $E_F$
IA	Half-metal	Metallic	Itinerant	None
IB	Half-metal	Metallic	None	Itinerant
IIA	Half-metal	Nonmetallic	Localized	None
IIB	Half-metal	Nonmetallic	None	Localized
IIIA	Metal	Metallic	Itinerant	Localized
IIIB	Metal	Metallic	Localized	Itinerant
IVA	Semimetal	Metallic	Itinerant	Localized
IVB	Semimetal	Metallic	Localized	Itinerant
VA	Semiconductor	Semiconducting	Few, itinerant	None
VB	Semiconductor	Semiconducting	None	Few, itinerant

units of the Bohr magneton. The integer spin moment criterion, or an extension of it to cover solid solutions, is a necessary but not a sufficient condition for half metallicity. Spin-orbit coupling is neglected; it may destroy half metallicity.<sup>1</sup>

Measuring the spin polarization is a key problem. Methods summarized in Fig. 3 are spin-polarized photoemission, and transport measurements in point contacts and tunnel junctions, either with two ferromagnetic electrodes, or with one ferromagnetic and one superconducting electrode.

The straightforward definition of spin polarization is

$$P_0 = (N^\uparrow - N^\downarrow) / (N^\uparrow + N^\downarrow), \quad (1)$$

where  $N^{\uparrow,\downarrow}$  are the densities of states at the Fermi level, but this is not necessarily what is measured. In experiments involving ballistic or diffusive transport, the densities of states must be weighted by  $v$  the Fermi velocity of the electrons, or its square, respectively,<sup>12</sup>

$$P_n = (\langle N^\uparrow v^{\uparrow n} \rangle - \langle N^\downarrow v^{\downarrow n} \rangle) / (\langle N^\uparrow v^{\uparrow n} \rangle + \langle N^\downarrow v^{\downarrow n} \rangle). \quad (2)$$

$P_1$  or  $P_2$  may be large for transport half metals (types III and IV), but  $P_0$  can be small for the same materials (Table II). The densities of states in tunnelling experiments should be weighted by the appropriate spin-dependent tunnelling matrix element to give  $P_T$ , which is equal to  $P_2$  for a specular barrier with low transparency.<sup>12</sup> There is mounting evidence that the spin polarization in a tunnel junction is critically dependent on the interface with the barrier, and can even change sign for a given ferromagnetic electrode according to the nature of the barrier.<sup>13</sup> If so, it makes little sense to talk about spin polarization as an intrinsic property of a material, unless  $P = 100\%$ .

Another difficulty arises when transport through the barrier does not occur in one step. Co-tunneling processes in-

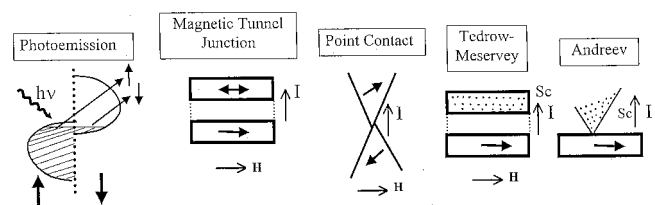


FIG. 3. Comparison of five methods of measuring  $P$ : Photoemission, tunnel junction, point contact, Tedrow-Meservey experiment, Andreev reflection.

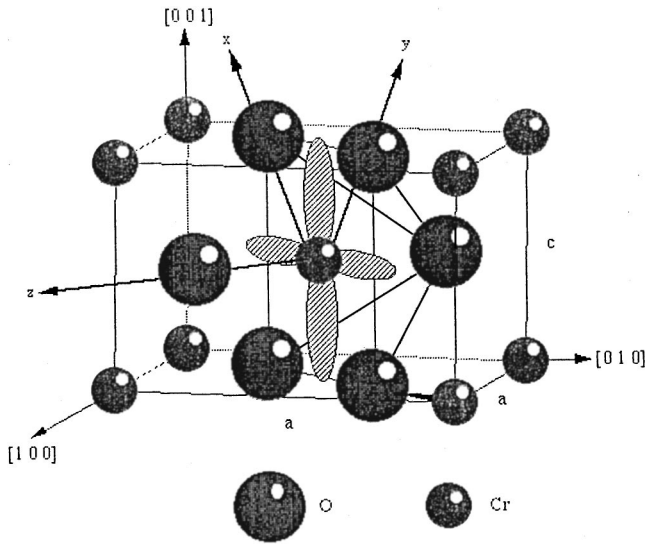


FIG. 4. The rutile structure of  $\text{CrO}_2$ . The local axis frame for the  $t_{2g}$  orbitals is shown.

volving intermediate states in the barrier are possible, and if the state involves a magnetic impurity, depolarization may occur.<sup>14</sup> Otherwise the polarization in a tunnel junction may be enhanced by multiple reflection in the barrier, or by transit via an intermediate state where there is Coulomb blockade.<sup>15</sup>

One would like to have a way of identifying a material as a half metal without the need to remove electrons. One possibility is to map the Fermi surface by measuring angular correlations of photons emitted following spin-polarized positron annihilation.<sup>16</sup> Otherwise, it might be possible to exploit the small shift in chemical potential  $g\mu_B B \approx 60 \mu\text{V T}^{-1}$ , that arises in an applied magnetic field. The authors are unaware of reports of any such measurements.

## II. CHROMIUM DIOXIDE

Chromium dioxide is the only stoichiometric binary oxide that is a ferromagnetic metal. It is the simplest and best-studied half metal.<sup>17</sup> Although metastable under ambient conditions, there is a narrow stability range near 300 °C which extends to high oxygen pressure. It has proved possible to grow small crystals and good-quality films, and produce powder which is sufficiently stable for industrial applications.<sup>18</sup> Acicular powder, typically  $100 \times 30 \times 30 \text{ nm}$ , is still used for video tapes. Thermal decomposition of  $\text{CrO}_3$  under natural oxygen pressure in a sealed vessel in the presence of a  $\text{TiO}_2$  substrate yields oriented thin films. Single-crystal films can be produced by chemical vapor transport of  $\text{CrO}_3$ ,  $\text{CrO}_2\text{Cl}_2$ , or  $\text{Cr}_8\text{O}_{21}$ ,<sup>19,20</sup> Photodecomposition of  $\text{Cr}(\text{CO})_6$  is another route.<sup>21</sup> The materials prepared in different ways do not necessarily have identical composition or properties. Substrate-induced strain in thin epitaxial films influences their physical properties.<sup>22</sup> Furthermore, the oxygen stoichiometry of thin films is usually undetermined. Early work on  $\text{CrO}_2$  is summarized in Chamberland's 1977 review.<sup>18</sup>

(a) *Structure and bonding*:  $\text{CrO}_2$  has the tetragonal rutile structure illustrated in Fig. 4. The space group is  $P4_2/\text{mnm}$

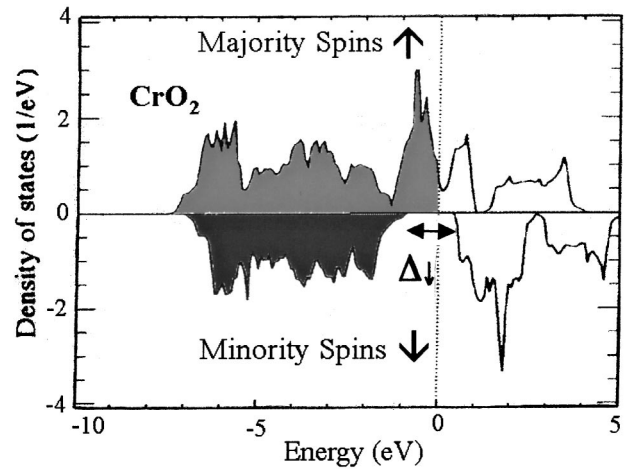


FIG. 5. Spin polarization of the density of states of  $\text{CrO}_2$  (Ref. 2).

with Cr in  $2a$  sites  $0,0,0; \frac{1}{2}, \frac{1}{2}, \frac{1}{2}$  and oxygen in  $4f$  sites  $\pm x, \pm x, 0; \frac{1}{2}\pm x, \frac{1}{2}\mp x, \frac{1}{2}$ , where  $x=0.302$ . Lattice parameters are  $a=0.4422 \text{ nm}$  and  $c=0.2917 \text{ nm}$ . Each oxygen has three chromium neighbors, and each chromium is octahedrally coordinated by oxygen with two short apical bonds (0.189 nm) and four longer equatorial bonds (0.191 nm). Octahedra sharing a common edge form ribbons parallel to  $c$ . Local axes are defined with  $x$  and  $y$  towards the edge-sharing oxygens, and  $z$  towards the apical oxygens. The Cr  $d$  orbitals are split by the crystal field ( $\sim 2.5 \text{ eV}$ ) into a  $t_{2g}$  triplet and an  $e_g$  doublet; the  $t_{2g}$  orbitals are split further into a nonbonding  $d_{xy}$  orbit which lies in the equatorial plane of the octahedron, and a  $d_{yz}, d_{zx}$  doublet, which form and antibonding  $d_{yz}\pm d_{zx}$  ( $\pi^*$ ) combinations with respect to the oxygen  $p$ -orbital perpendicular to the  $\text{Cr}_3\text{O}$  triangles.<sup>23,24</sup>

(b) *Electronic structure*: The formal electronic configuration is  $(t_{2g}^2)^{\uparrow}$  for  $\text{Cr}^{4+}$ , and  $2p^6$  for  $\text{O}^{2-}$  although there is some  $\text{O}^{2-} \rightarrow \text{Cr}^{4+}$  charge transfer and strong mixing of oxygen hole and chromium electron states at  $E_F$ .<sup>25</sup> The Cr  $d$  levels lie close to the top of the O  $2p$  band. The Fermi level lies in the half-full  $d_{yz}\pm d_{zx}$  band. A dozen LSDA, LSDA +U, and GCA calculations, beginning with that of Schwarz<sup>26</sup> have refined the picture. There is a large peak in the paramagnetic density of states at  $E_F$ , but almost every calculation confirms that the spin-split band structure is that of a type IA half metal, with a spin gap  $\Delta_1 > 1 \text{ eV}$ , and a spin-flip gap  $\Delta_{sf}$  of a few tenths of an eV (Table III). The calculations generally show a  $t_{2g}$  bandwidth of 2.5 eV, with a trident structure including a narrow peak in the density of

TABLE II. Calculated spin polarization in ferromagnetic oxides.

	$\text{CrO}_2$ (Ref. 2)	$(\text{La}_{0.67}\text{Ca}_{0.33})\text{MnO}_3$ (Ref. 7)	$\text{Ti}_2\text{Mn}_2\text{O}_7$ (Ref. 8)
$N^{\uparrow}$ ( $\text{eV}^{-1} \text{ f.u.}^{-1}$ )	0.69	0.58	1.25
$N^{\downarrow}$ ( $\text{eV}^{-1} \text{ f.u.}^{-1}$ )		0.27	0.24
$V_F^{\uparrow}$ ( $10^6 \text{ ms}^{-1}$ )	0.25	0.76	0.06
$V_F^{\downarrow}$ ( $10^6 \text{ ms}^{-1}$ )		0.22	0.33
$P_0$ %	100	36	66
$P_1$ %	100	76	-5
$P_2$ %	100	92	-71

states due to the  $d_{xy}$  electrons (Fig. 5). The Fermi level lies in a pseudogap between the  $d_{yz} \pm d_{zx}$  bands, but its position relative to the minimum is rather sensitive to details of the calculation. The half-metallic character is maintained up to the surface.<sup>27</sup> There is controversy about the screening of the on-site Coulomb correlations  $U$ , with magneto-optic spectra suggesting effective screening<sup>28</sup> while core level spectroscopy and photoemission suggest the opposite.<sup>29,30</sup> All the calculations yield a moment very close to  $2 \mu_B$ /formula. Both Cr electrons and Cr/O holes are present at  $E_F$ . The Fermi surface presents two main features;<sup>31,32</sup> an electron pseudocube centered at the  $\Gamma$  point which contains 0.12 electrons f.u.<sup>-1</sup>, and a compensating hole surface centered near Z, whose shape is extremely sensitive to the position of the Fermi level. There may be small extra electron and hole pockets.<sup>32</sup>

(c) *Magnetic properties:* The Curie temperature of  $\text{CrO}_2$  is usually reported to lie in the range 392(6) K. The critical behavior of an epitaxial film with  $T_C = 386.5$  K is that of a normal Heisenberg ferromagnet with  $\beta = 0.371$  and  $\gamma = 1.43$ .<sup>33</sup> The low temperature ferromagnetic moment  $\sigma = 133 \text{ Am}^2/\text{kg}$  ( $J = 0.824$  T) corresponds to an integral moment of  $2.0 \mu_B/\text{f.u.}$ ,<sup>18</sup> as expected for a half metal. Nevertheless, there is evidence that the Cr moment is actually closer to  $2.1 \mu_B/\text{f.u.}$  with a compensating moment of  $-0.1 \mu_B/\text{f.u.}$  on the oxygen, reflecting the covalent mixing of Cr  $t_{2g}^{\uparrow}$  and O  $2p$  states.<sup>17,34,35</sup>

The temperature dependence of the magnetization well below  $T_C$  follows a Bloch  $T^{3/2}$  law<sup>36</sup> with spin wave stiffness  $D \approx 1.8 \times 10^{-40} \text{ J m}^2$ , indicating that normal ferromagnetic spin waves are excited. They are detected by ferromagnetic resonance in thin films, where the Gilbert damping parameter is very small.<sup>37</sup> The localized  $S = \frac{1}{2}$ ,  $d_{xy}$  core is exchange coupled to the ( $d_{yz} + d_{zx}$ ) conduction electrons by an on-site Hund's rule interaction  $J_H \sim 1 \text{ eV}$  to form  $S = 1$  atomic spins, which then interact by double-exchange and ferromagnetic superexchange interactions. The intrinsic magnetocrystalline anisotropy of epitaxial  $\text{CrO}_2$  films on (100)  $\text{TiO}_2$  is  $K_1 = 27 \text{ kJ/m}^3$  at room temperature, with an easy  $c$  axis.<sup>38</sup> In powders, the easy axis is reported to lie at about  $20^\circ$  to  $\mathbf{c}$ .<sup>34</sup> Shape anisotropy for acicular particles used in magnetic recording may be as high as  $\mu_0 M_S^2/4$ , giving  $K_S \approx 50 \text{ kJ/m}^3$  at room temperature. Magnetostriction is  $\lambda_S = 5 \times 10^{-6}$ .<sup>39</sup>

The paramagnetic moment deduced from the Curie-Weiss susceptibility above  $T_C$  slightly exceeds that expected for  $S = 1$ .<sup>17,18</sup> There is no evidence that it is much less than  $g\sqrt{[S(S+1)]}\mu_B$ , as had been predicted for a half metal.<sup>40</sup>

(d) *Thermal properties:* The low temperature heat capacity of sintered<sup>29</sup> and powdered  $\text{CrO}_2$ <sup>36</sup> has been fitted to yield values of the electronic term  $\gamma = 2.5 \text{ mJ/mol K}^2$  and  $5.1 \text{ mJ/mol K}^2$ , respectively, which are typical of  $d$ -band ferromagnets. The corresponding densities of states,  $N^{\uparrow} = 1.1$  and  $2.2 \text{ eV}^{-1} \text{ f.u.}^{-1}$ , are enhanced relative to the calculated values given in Table III. The enhancement may be explained by electron-phonon<sup>2</sup> and correlation effects.<sup>40</sup> The spin-wave specific heat, varying as  $T^{3/2}$ , is enhanced with respect to the value deduced from the Bloch law, which corresponds to  $D \approx 1.1 \times 10^{-40} \text{ J m}^2$ .<sup>17,29</sup> The Debye temperature deduced

TABLE III. Some electronic structure calculation on  $\text{CrO}_2$ .

Author		$\Delta_{\downarrow}$ (eV)	$\Delta_{\text{sf}}$ (eV)	$N_{\uparrow} \text{ eV}^{-1} \text{ f.u.}^{-1}$
Schwarz	Ref. 26 LSDA-ASW	1.3	0.3	0.8
Lewis <i>et al.</i>	Ref. 2 LSDA-PWPP	1.4	0.3	0.69
Korotin <i>et al.</i>	Ref. 27 LSDA+U(3 eV)	2.4	1.7	0.4
Mazin <i>et al.</i>	Ref. 31 LSDA/GGA	1.3	0.2-0.7	0.95
Brener <i>et al.</i>	Ref. 32 LSDA-LCGO	1.3	0.2	1.16
Kuneš <i>et al.</i>	Ref. 28 GGA	1.8	0.7	0.3

from the low temperature heat capacity is 593 K. The Seebeck coefficient is  $\approx -10 \mu\text{V K}^{-1}$ .<sup>18</sup>

(e) *Spectroscopic properties:* Optical reflectivity data are available as a function of temperature.<sup>41</sup> In the optical conductivity, there is a strong temperature-dependent Drude peak at low frequency and features at 2.0 and 3.0 eV which are assigned to intraband transitions across the pseudogap, and interband transitions across the spin gap  $\Delta_{\downarrow}$ , respectively. Spin-flip excitations occur in the range 0.06-0.25 eV where there is a rapid decrease in relaxation rate at low temperature.<sup>41</sup> Using a calculated plasma frequency  $\omega_p = 17000 \text{ cm}^{-1}$  and Fermi velocity  $v_F = 0.25 \times 10^6 \text{ ms}^{-1}$ ,<sup>2</sup> the relaxation rate at 10 K and zero frequency,  $13 \text{ cm}^{-1}$ , corresponds to a mean free path of 115 nm. The low-frequency scattering rate increases by more than a factor 100 between 10 K and 300 K. Off-diagonal optical conductivity, deduced from the frequency dependence of the Faraday and Kerr effect agrees well with GGA calculations by Kuneš.<sup>28</sup> Broadening of Raman modes near  $T_C$  is associated with scattering from collective spin fluctuations.<sup>42</sup> The energy of the  $A_{1g}$  mode agrees well with the LSDA calculation.<sup>2</sup> Photoemission studies show a small density of states at  $E_F$ .<sup>29</sup>

(f) *Transport properties (intrinsic):* The electrical conductivity determined on single crystals or high quality films shows residual resistivity  $\rho_0$  of a few  $10^{-8} \Omega\text{m}$ <sup>17,18,43,44</sup> and a resistivity ratio  $\rho(300 \text{ K})/\rho_0$  that can be as high as 140.<sup>22</sup> Below 50 K,  $\text{CrO}_2$  is a rather good metal, with a resistivity that is practically independent of temperature (Fig. 6). The mean free path corresponding to  $\rho_0 = 4 \times 10^{-8} \Omega\text{m}$  is  $\approx 90 \text{ nm}$ .<sup>2</sup> The resistivity continues to increase at high temperatures, with a change of slope of  $d\rho/dT$  at  $T_C$ , reaching  $6 \mu\Omega\text{m}$  or more. Based on the area of the paramagnetic Fermi surface,<sup>2</sup> this implies a mean free path of 0.1 nm, making  $\text{CrO}_2$  a bad metal in the sense that  $d\rho/dT > 0$ . However, if the spin splitting persists above  $T_C$ , the mean free path there is then  $\approx 0.5 \text{ nm}$ , which is a bit more than the interatomic spacing. The sign of  $d\rho/dT$  above  $T_C$  becomes negative at high frequency.<sup>45</sup> The scattering of magnetic origin, estimated by extrapolating the high field slope to zero is  $2.8 \mu\Omega\text{m}$ .<sup>17</sup>

Suppression of the normal ferromagnetic  $T^2$  scattering at low temperature, together with intense magnetic scattering at higher temperatures leads to a resistivity varying as  $\rho = \rho_0 + AT^2 e^{-\Delta/T}$  where  $A \approx 33 \Omega\text{m/K}^2$  and  $\Delta \approx 80 \text{ K}$ . Data have also been fitted to a simple power law  $\rho \propto T^n$ , where  $n = 3$ .<sup>2,44</sup>  $\Delta$  is much less than  $\Delta_{\text{sf}}$  (Table III). Spin-wave scattering appears only to be effective for magnon wavelengths shorter than a threshold corresponding to this energy (3 nm).<sup>36</sup>

The change in conduction regime at low temperature is evident in the magnetoresistance.<sup>43,44,46</sup> The intrinsic proper-

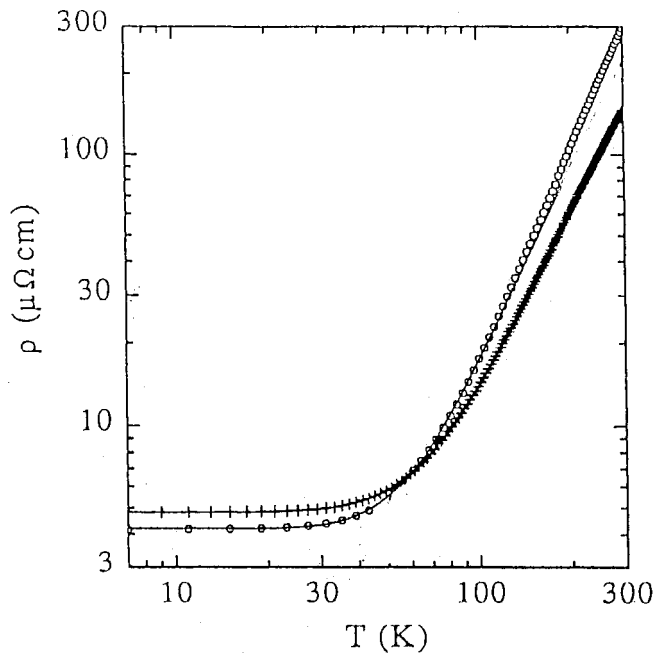


FIG. 6. Resistivity of CrO<sub>2</sub> thin films (Ref. 43).

ties are best seen in unstrained films with little residual resistivity. Above 300 K, the magnetoresistance is negative, linear, and isotropic with a value of order 1%/T.<sup>47</sup> Its origin is the reduction of spin-disorder scattering by the field-induced magnetization. At low temperatures, large positive perpendicular (field perpendicular to film) and transverse (field parallel to film) magnetoresistance varies as  $B^2$  reflecting<sup>43,44</sup> high mobility and long mean free path of the carriers.

The Hall effect in CrO<sub>2</sub> is the sum of the ordinary and anomalous terms  $\rho_H = R_0 B + R_S \mu_0 M$ . The anomalous term dominates the Hall resistivity above 150 K;  $R_S$  varies as  $T^4$  from 40–300 K, indicating a side-jump mechanism for which  $R_S \propto \rho^2$ .<sup>43</sup> The normal Hall effect is the predominant contribution below 80 K.<sup>43,48</sup> Notable is the change of the slope from positive to negative beyond a value of applied field which depends sensitively on sample preparation. Interpreted in a simple two-band model, the positive slope at low fields reflects the presence of highly mobile holes, which pass over to the high field condition  $\omega_c \tau = \mu B > 1$  above the turning field, where  $\mu$  is the mobility. The Hall effect is then dominated by the more numerous electrons. The two-band analysis gives  $\mu_n = 0.25 \text{ T}^{-1}$ , and  $\mu_e = 0.01 \text{ T}^{-1}$ . Both mobilities have the same temperature dependence,  $\mu(0)/\mu(T) = 1 + AT^2 e^{-\Delta/T}$  with  $\Delta = 80 \text{ K}$ .<sup>43</sup> The two band analysis is a simplification in view of the complex Fermi surface, but the essential feature is mobile holes, of O ( $2p$ ) character and heavy Cr( $t_{2g}$ ) electrons (and holes).

(g) *Transport properties (extrinsic)*: The extrinsic transport properties have been studied in tunnel junctions, polycrystalline films, pressed powders and point contacts. The natural barrier oxide on CrO<sub>2</sub> is 2–3 nm of Cr<sub>2</sub>O<sub>3</sub>,<sup>49</sup> an antiferromagnet with  $T_N = 300 \text{ K}$ . CrO<sub>2</sub>/native oxide/Co junctions exhibited disappointingly small magnetoresistance, 1% at 77 K and 8% at 4.2 K, of either sign.<sup>50,51</sup> Granular

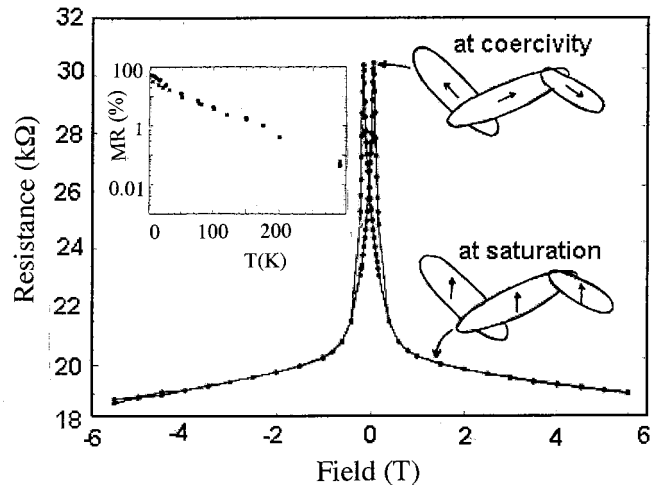


FIG. 7. Magnetoresistance of a CrO<sub>2</sub>–Cr<sub>2</sub>O<sub>3</sub> pressed powder compact, with temperature dependence shown in the inset (Ref. 56).

films<sup>52</sup> and powder compacts<sup>53–55</sup> show larger effects.

Powder magnetoresistance is a simple and versatile method for investigating magnetotransport in half metals.<sup>56</sup> Ideally, the transmission  $T$  of electrons across a tunnel barrier between two misaligned half-metallic particles whose magnetic axes are at an angle  $\theta_{ij}$  varies as  $\cos^2(\theta_{ij}/2)$ , which is identical to  $(1 + \cos \theta_{ij})/2$ . If the directions of magnetization of the particles are random ( $r$ ),  $\langle \cos \theta_{ij} \rangle = 0$ , and the maximum observable magnetoresistance,

$$\text{MR} = (\sigma_{\parallel} - \sigma_r) / \sigma_{\parallel} = (\rho_r - \rho_{\parallel}) / \rho_r \quad (3)$$

is 50%. Since  $\langle \cos \theta_{ij} \rangle = \langle \cos \theta_{ij} \rangle^2 = m^2$ , this reduces to  $m^2 / (1 + m^2)$  if the moments are incompletely aligned in the  $\parallel$  state. The pressed powders show hysteretic, butterfly-shaped magnetoresistance curves which do not saturate easily (Fig. 7). Taking  $\rho_{\parallel}$  as the extrapolated value for  $1/H \rightarrow 0$  and  $\rho_r$  as the maximum gives  $\text{MR} = 31\%$  at 4.2 K.<sup>49,53</sup> For imperfect polarization, the transmission varies as  $P^2 \cos^2(\theta_{ij}/2)$ , which gives  $\text{MR} = P^2 / (1 + P^2)$ , hence  $P = 67\%$ . This is an underestimate for two reasons (i) the resistance is greater in the virgin unmagnetized state than it is at the coercive field, so that  $\langle \cos \theta_{ij} \rangle > 0$  at coercivity, (ii) there is a nonzero transmission probability when the electrodes are antiparallel, associated with spin-wave excitations. The magnetoresistance on an aligned powder is greater than 41%,<sup>55</sup> but still far from 100% as might be expected if the acicular CrO<sub>2</sub> powder particles all had antiparallel neighbors at the coercive field. However, the experimentally determined percolation fraction for these particles is 0.23,<sup>53</sup> so there will always be a percolation path through a 50–50 mixture of  $\uparrow$  and  $\downarrow$  particles.

Dilution of the CrO<sub>2</sub> with Cr<sub>2</sub>O<sub>3</sub> particles (Fig. 7) increases the resistance and the magnetoresistance. Close to the percolation threshold, the magnetoresistance extrapolated to  $T = 0$  and  $1/H = 0$  rises to 40% which would correspond to  $P = 82\%$ . However, there is a low temperature upturn in  $\rho$  of the form  $\rho \sim \exp(\Delta'/T)^{1/2}$  (Refs. 44, 53, and 55) which is due to Coulomb blockade. The barrier  $\Delta'$  is magnetization dependent and the magnetoresistance increases in this regime be-

cause the electrons find more eligible particles to which they can tunnel when the magnetization is aligned.

Finally, a series of Andreev experiments<sup>57–60</sup> have been carried out on CrO<sub>2</sub>–superconductor point contacts and pin-hole junctions. These indicate a very high spin polarization,  $P \approx 80\%–97\%$  for CrO<sub>2</sub> in the 1 K temperature range. Most convincing evidence of complete spin polarization is seen in a recent Tedrow–Meservey experiment using CrO<sub>2</sub> with a specially prepared Cr<sub>2</sub>O<sub>3</sub> barrier and a Pb counterelectrode.<sup>60</sup>

### III. CONCLUSIONS

The concept of half metallicity has been extended with examples of most of the new types, being based on electronic structure calculations. It is not easy to identify any material as a half-metal experimentally. The discussion of CrO<sub>2</sub> has highlighted measurements of spin polarization at low temperatures using superconducting electrodes or powder magnetoresistance. The transport properties exhibit a syndrome where spin–flip scattering seems to be suppressed below a temperature  $\Delta \approx 0.2 T_C$ . This is related somehow to spin–wave excitations and not to the spin–flip gap  $\Delta_{sf}$ , which is many times greater than  $\Delta$ .

The band structure of half metals is especially sensitive to spin disorder, which reduces the transfer integral and narrows the bandwidth in a static picture.<sup>61</sup> This may lead to instantaneous localization, which is relieved by favorable spin fluctuations in the atomic nearest-neighbor environment giving rise to bad metal behavior near and above  $T_C$ .

It is a challenge to measure and explain the intrinsic temperature dependence of the spin polarization of half metals, and ultimately to exploit them in spin electronics.

### ACKNOWLEDGMENTS

This work was supported by the Science Foundation of Ireland.

- <sup>1</sup>H. Eschrig and W. E. Pickett, *Solid State Commun.* **118**, 123 (2001).
- <sup>2</sup>S. P. Lewis, P. B. Allen, and T. Sasaki, *Phys. Rev. B* **55**, 10253 (1997).
- <sup>3</sup>R. A. de Groot, F. M. Mueller, P. G. van Engen, and K. H. J. Buschow, *Phys. Rev. Lett.* **50**, 2024 (1983).
- <sup>4</sup>K. I. Kobayashi, T. Kimura, H. Sawada, K. Terakura, and Y. Tokura, *Nature (London)* **395**, 677 (1998).
- <sup>5</sup>R. Weht and W. E. Pickett, *Phys. Rev. B* **60**, 13006 (1999).
- <sup>6</sup>M. Penicaud, B. Silberchiot, C. B. Sommers, and J. Kubler, *J. Magn. Magn. Mater.* **103**, 212 (1992).
- <sup>7</sup>B. Nadgorny, I. I. Mazin, M. Osofsky, R. J. Soulen, P. Broussard, R. M. Stroud, D. J. Singh, V. G. Harris, A. Arsenov, and Ya Mukovskii, *Phys. Rev. B* **63**, 18 4433 (2001).
- <sup>8</sup>D. J. Singh, *Phys. Rev. B* **55**, 313 (1997).
- <sup>9</sup>F. Holtzberg, S. von Molnar, and J. M. D. Coey, in *Handbook of Semiconductors*, edited by S. P. Keller Vol. 3, Chap. 13 (1980).
- <sup>10</sup>S. Sanvito, P. Ordejon, and N. A. Hill, *Phys. Rev. B* **63**, 165206 (2001).
- <sup>11</sup>I. I. Mazin, *Appl. Phys. Lett.* **77**, 3000 (2000).
- <sup>12</sup>I. I. Mazin, *Phys. Rev. Lett.* **83**, 1427 (1999).
- <sup>13</sup>J. M. De Teresa, A. Bathélemy, A. Fert, J. P. Contour, R. Lyonnet, F. Montaigne, P. Seneor, and A. Vaures, *Phys. Rev. Lett.* **82**, 4288 (1999).
- <sup>14</sup>P. Guinea, *Phys. Rev. B* **58**, 9212 (1998).
- <sup>15</sup>S. Takahashi and S. Maekawa, *Phys. Rev. Lett.* **81**, 2799 (1998).
- <sup>16</sup>K. Hanssen, P. E. Mijnders, L. P. L. M. Rabou, and K. H. J. Buschow, *Phys. Rev. B* **42**, 1533 (1990).
- <sup>17</sup>A. Barry, Ph.D. thesis, Trinity College, University of Dublin, 1999.

- <sup>18</sup>B. L. Chamberland, *CRC Crit. Rev. Solid State Mater. Sci.* **7**, 1 (1977).
- <sup>19</sup>X. W. Li, A. Gupta, T. R. McGuire, P. R. Duncombe, and G. Xiao, *J. Appl. Phys.* **85**, 5585 (1999).
- <sup>20</sup>P. G. Ivanov, S. M. Watts, and D. M. Lind, *J. Appl. Phys.* **89**, 1035 (2001).
- <sup>21</sup>P. A. Dowben, Y. G. Kim, S. Baral-Tosh, G. O. Ramseyer, C. Hwang, and M. Onellion, *J. Appl. Phys.* **67**, 5658 (1990).
- <sup>22</sup>P. A. Stampe, R. J. Kennedy, S. M. Watts, and S. von Molnar, *J. Appl. Phys.* **89**, 7696 (2001).
- <sup>23</sup>J. B. Goodenough, *Prog. Solid State Chem.* **5**, 235 (1971).
- <sup>24</sup>P. I. Sorantin and K. Schwartz, *Inorg. Chem.* **31**, 567 (1992).
- <sup>25</sup>M. A. Korotin, V. I. Anisimov, D. I. Khomski, and G. A. Sawatzky, *Phys. Rev. Lett.* **80**, 4305 (1998).
- <sup>26</sup>K. Schwarz, *J. Phys. F: Met. Phys.* **16**, L211 (1986).
- <sup>27</sup>H. van Leuken and R. A. de Groot, *Phys. Rev. B* **51**, 7176 (1995).
- <sup>28</sup>J. Kunes, P. Novák, P. M. Oppeneer, C. König, M. Fraune, U. Rüdiger, G. Güntherodt, and C. Ambrosch-Draxl (unpublished).
- <sup>29</sup>T. Tsujioka, T. Mizokawa, J. Okamoto, A. Fujimori, M. Nohara, H. Takagi, K. Yamaura, and M. Takana, *Phys. Rev. B* **56**, R15 509 (1997).
- <sup>30</sup>C. B. Stagaescu, X. Su, D. E. Eastman, K. N. Altmann, F. J. Himpsel, and A. Gupta, *Phys. Rev. B* **61**, R9233 (2000).
- <sup>31</sup>I. I. Mazin, D. J. Singh, and C. Ambrosch-Draxl, *Phys. Rev. B* **59**, 411 (1999).
- <sup>32</sup>N. E. Brener, J. M. Tyler, J. Callaway, D. Bagayoko, and G. L. Zhao, *Phys. Rev. B* **61**, 16582 (2000).
- <sup>33</sup>F. Y. Yang, C. L. Chien, X. W. Li, G. Xiao, and A. Gupta, *Phys. Rev. B* **63**, 092403 (2001).
- <sup>34</sup>J. K. Burdett, G. J. Miller, J. W. Richardson, Jr., and J. V. Smith, *J. Am. Chem. Soc.* **110**, 8064 (1988).
- <sup>35</sup>K. Attenkofer and G. Schütz, *J. Phys. IV* **7**, C2459 (1997).
- <sup>36</sup>A. Barry, J. M. D. Coey, L. Ranno, and K. Ounadjela, *J. Appl. Phys.* **83**, 7166 (1998).
- <sup>37</sup>P. Lubitz, M. Rubinstein, M. S. Osofsky, B. E. Nadgorny, R. J. Soulen, K. M. Bussmann, and A. Gupta, *J. Appl. Phys.* **89**, 6695 (2001).
- <sup>38</sup>F. Y. Yang, C. L. Chien, E. F. Ferrari, X. W. Li, G. Xiao, and A. Gupta, *Appl. Phys. Lett.* **77**, 286 (2000).
- <sup>39</sup>X. W. Li, A. Gupta, and G. Xiao, *Appl. Phys. Lett.* **75**, 713 (1999).
- <sup>40</sup>V. Yu. Irkhin and M. I. Katsnel'son, *Sov. Phys. Usp.* **37**, 659 (1994).
- <sup>41</sup>E. J. Singley, C. P. Weber, D. N. Basov, A. Barry, and J. M. D. Coey, *Phys. Rev. B* **60**, 4126 (1999).
- <sup>42</sup>M. N. Iliiev, A. P. Litvinchuk, H.-G. Lee, C. W. Chu, A. Barry, and J. M. D. Coey, *Phys. Rev. B* **60**, 33 (1999).
- <sup>43</sup>S. M. Watts, S. Wirth, S. von Molnar, A. Barry, and J. M. D. Coey, *Phys. Rev. B* **61**, 149621 (2000).
- <sup>44</sup>A. Gupta, X. W. Li, and G. Xiao, *J. Appl. Phys.* **87**, 6073 (2000).
- <sup>45</sup>C. M. Fu, C. J. Lai, J. S. Wu, J. C. A. Huang, C.-C. Wu, and S.-G. Shyu, *J. Appl. Phys.* **89**, 7702 (2001).
- <sup>46</sup>K. Suzuki and P. M. Tedrow, *Phys. Rev. B* **58**, 11 597 (1998).
- <sup>47</sup>U. Rüdiger, M. Rabe, K. Samm, B. Özyilmaz, J. Pommer, M. Fraune, G. Güntherodt, St. Senz, and D. Hesse, *J. Appl. Phys.* **89**, 7699 (2001).
- <sup>48</sup>X. W. Li, A. Gupta, T. R. McGuire, P. R. Duncombe, and G. Xiao, *J. Appl. Phys.* **85**, 5585 (1999).
- <sup>49</sup>J.-B. Dai, J.-K. Tang, H.-P. Xu, L. Spinu, W.-D. Wang, K. Y. Wang, A. Kumbhar, M. Li, and U. Diebold, *Appl. Phys. Lett.* **77**, 2840 (2000).
- <sup>50</sup>A. Barry, J. M. D. Coey, and M. Viret, *J. Phys.: Condens. Matter* **12**, L173 (2000).
- <sup>51</sup>A. Gupta, X. W. Li, and G. Xiao, *Appl. Phys. Lett.* **78**, 1894 (2001).
- <sup>52</sup>H. Y. Hwang and S. W. Cheong, *Science* **278**, 1607 (1997).
- <sup>53</sup>J. M. D. Coey, A. E. Berkowitz, L. I. Balcells, and F. F. Purtil, and A. Barry, *Phys. Rev. Lett.* **80**, 3815 (1998).
- <sup>54</sup>S. S. Manoharan, D. Elefant, G. Reiss, and J. B. Goodenough, *Appl. Phys. Lett.* **72**, 984 (1998).
- <sup>55</sup>J.-B. Dai and J. Tang, *Phys. Rev. B* **63**, 054434 (2001).
- <sup>56</sup>J. M. D. Coey, *J. Appl. Phys.* **85**, 5576 (1999).
- <sup>57</sup>R. J. Soulen *et al.*, *Science* **282**, 85 (1998).
- <sup>58</sup>W. J. De Sisto, P. R. Broussard, T. F. Ambrose, B. E. Nadgorny, and M. S. Osofsky, *Appl. Phys. Lett.* **76**, 3789 (2000).
- <sup>59</sup>Y. Ji, G. J. Strijkers, F. Y. Yang, C. L. Chien, J. M. Byers, A. Anguelouch, G. Xiao, and A. Gupta, *Phys. Rev. Lett.* **86**, 5585 (2001).
- <sup>60</sup>J. S. Parker, S. M. Watts, P. G. Ivanov, and P. Xiong (unpublished).
- <sup>61</sup>S. H. Liu, *J. Magn. Magn. Mater.* **212**, 259 (2000).